JOURNAL OF PROPULSION AND POWER
Vol. 13, No. 1, January–February 1997

Multidimensional Modeling of Fuel Effects and Split Injections on Diesel Engine Cold-Starting

Nabil S. Ayoub* and Rolf D. Reitz†
University of Wisconsin, Madison, Wisconsin 53706

A computational model has been developed for describing multicomponent fuel vaporization and ignition in diesel engines and was implemented in the KIVA-II computational fluid dynamics code. The model has been applied to understand diesel engine cold-starting and the parameters that significantly influence this phenomena. Typical diesel fuels are blends of various fuels species, i.e., multicomponent. Thus, the original single-component fuel vaporization model in KIVA-II was replaced by a multicomponent fuel vaporization model. Necessary modifications were carried out in other spray submodels that describe droplet breakup and coalescence to account for multicomponent fuels. The autoignition process was modeled using a modified multistep kinetics Shell ignition model to account for fuel composition effects. The improved model was applied to simulate cold-starting in diesel engines. The effects of fuel residual left from previous cycles, injection timing, and duration were studied. Split injections, where a small pilot injection was introduced during the compression stroke, were found to have a significant and beneficial effect on cold-starting.

Nomenclature

a = Redlich–Kwong constant
B_0 = drop size constant
B_1 = breakup time constant
b = Redlich–Kwong constant
C = internal mixing factor
C_D = coefficient of drag
D = mass diffusivity
E_a = activation energy
f = fugacity, delay coefficient
$f°$ = fugacity at standard state
K = reaction rate constant
k = turbulent kinetic energy
k_{ij} = binary interaction coefficient
n = number of components
P = pressure
R = universal gas constant
r = droplet radius
T = temperature
t = time
U = drop-gas relative velocity
v = specific volume
X = liquid mole fraction
$\boldsymbol{x}$ = droplet position vector, displacement
Y = vapor mole fraction
y = droplet distortion parameter
z = compressibility factor
γ = activity coefficient
ε = turbulent kinetic energy dissipation rate
Λ = wavelength
μ = dynamic viscosity
σ = surface tension coefficient
τ = characteristic time
ϕ = deviation from ideal gas behavior
Ω = Redlich–Kwong constant, wave growth rate
ω = acentric factor

Subscripts
c = critical properties
g = gas phase
i, j = index for fuel components
l = laminar, liquid phase
s = surface of droplet
t = turbulent
12 = liquid fuel components

Superscripts
l = liquid phase
v = vapor phase
° = reference state

Introduction

RECENT concerns about the environment, together with a significant increase in the number of diesel engines that provide automotive power, have resulted in the introduction of more legislation to limit their pollutant emissions, particularly nitrogen oxides (NO_x) and soot emissions. Both of these pollutants are influenced significantly by both the fuel and the injection system. Also, a considerable fraction of other pollutant emissions, particularly unburned hydrocarbons, is produced during engine cold-starting. Thus, the trend to lower emissions while improving engine performance has motivated significant research efforts, both computationally and experimentally.

Furthermore, starting the diesel engine under cold ambient conditions represents a difficulty in itself. More research is needed to identify mechanisms that would improve the startability of the engine under such conditions. Cold-starting is characterized as a situation where the engine misfires for several cycles, or fires for one cycle and skips firing for several cycles to follow.[1] There are several other issues of importance in cold-starting of diesel engines,[2] such as fuel carryover from misfiring and borderline cycles, excessive wear from high-peak pressures reached after combustion that follows misfiring, and the increase of blowby gases at slower cranking speeds that further reduces compression temperatures. Finally, the issue of unburned hydrocarbons and white smoke contributes significantly to the engine emissions.

Received Dec. 12, 1995; revision received June 10, 1996; accepted for publication June 12, 1996.

*Graduate Student, Engine Research Center, Mechanical Engineering Department, 1500 Engineering Drive.

†Professor, Engine Research Center, Mechanical Engineering Department, 1500 Engineering Drive.

The controlling processes that govern diesel engine performance are very complicated and need to be broken down to several distinct subprocesses such as injection, atomization, vaporization, ignition, and combustion, etc. Once each process is investigated, a comprehensive understanding of diesel combustion can be achieved. For combustion to start in a fuel spray, the droplets must vaporize to some extent. Thus, the ignition delay (the delay time between the start of injection and ignition), as well as the rate of combustion, are strong functions of the droplet vaporization rate.[3] Multicomponent fuel vaporization models have been extensively discussed,[4] and results have been presented for single droplets with comparison to experimental data, for sprays and several engine cases.

The objective of this work is to understand the process of cold-starting and to explore various parameters that can help improve the cold-startability of the engine using advanced computational models.

Theoretical Model

The KIVA-II code[5] was used in this study with improvements in the spray, ignition, combustion, and emission models. The code solves the mass, momentum, and energy conservation equations, coupled with the k-ε turbulence model in three dimensions as a function of time. The interactions between the spray droplets and the gas phase are also accounted for. Since the governing equations in the KIVA-II code are documented,[5] only the improved submodels will be discussed. Other improvements in the wall heat transfer and spray-wall impingement models that were also incorporated in the present study have already been discussed.[2,6,7] Flow through the piston–cylinder–ring crevice was also accounted for by using a phenomenological crevice flow model[7,8] that was coupled to the KIVA solution.

Droplet Vaporization

The multicomponent fuel vaporization model[9] was implemented in the KIVA-II code in the present study. This model is a comprehensive model that handles high-pressure effects in multicomponent fuel vaporization. The basic assumptions in this model are, droplets are spherically symmetric, pressure is uniform in space around the droplet, the gas–liquid interface is in thermodynamic equilibrium, no cross effects exist between heat and mass transfer, and gas is dissolved in a very thin liquid surface layer (i.e., gas does not diffuse into the droplet interior).

This model not only accounts for high-pressure effects, but it also takes into consideration the following nonideal phenomena: variable gas and liquid properties, nonideal gas effects at the droplet interface, high-mass-transfer corrections on heat and mass transfer, heat and mass diffusion inside the droplet, and internal mixing effects.

To achieve equilibrium in a multicomponent multiphase system, the fugacities of each of the n components have to be equal in both the liquid and gas phases: $f_i^v = f_i^l$, where $i = 1, \ldots, n$. In the present model, the ambient gas is considered as a component in the system. However, the presence of the gas species in the liquid phase is limited to a thin surface layer on the droplet.[9]

To calculate the gas-phase fugacities, the Redlich–Kwong equation of state is used

$$P = \frac{RT}{v - b} - \frac{a}{T^{0.5}v(v + b)}$$

where v is the volume of the gas mixture, and the constants a and b are to be evaluated by mixing rules in multicomponent gas mixtures.[10] The use of the ideal gas law is adequate at the outer edge of the gas boundary layer because the species concentrations are typically much less than at the droplet surface. Therefore, the approximation of using the ideal gas equation at the edge of the boundary layer matches the ideal equation of state that is used in the KIVA-II code. By definition, the gas phase fugacity for component i is given by $f_i^v = \phi_i P Y_{is}$, and as ϕ_i approaches unity, the vapor phase fugacity is exactly equivalent to the vapor pressure. This approximation is called Raoult's law,[10] and it is only applicable under near-atmospheric pressures in nearly ideal solutions; in mixtures where one component is in large excess (e.g., 90%); and in mixtures with components of similar properties.

The fugacity coefficient f_i is a function of the pressure, temperature, and gas composition, and is expressed by

$$RT\ \ell n(\phi_i) = \int_{V_0}^{V} \left(\left.\frac{\partial P}{\partial n_i}\right|_{T,V,n_j} - \frac{RT}{V} \right) \mathrm{d}V - RT\ \ell n(z) \quad (1)$$

where z is the compressibility of the gas mixture at T and P. In Eq. (1), the mixing rules are

$$b = \sum_i y_i b_i \quad \text{where} \quad b_i = \frac{\Omega_{b_i} R T_{c_i}}{P_{c_i}}$$

$$a = \sum_i \sum_j y_i y_j a_{ij} \quad \text{where} \quad a_{ii} = \frac{\Omega_{a_i} R^2 T_{c_i}^{2.5}}{P_{c_i}}$$

$$a_{ij} = \frac{(\Omega_{a_i} + \Omega_{a_j}) R^2 T_{c_{ij}}^{2.5}}{2P_{c_{ij}}}$$

The subscript c denotes critical properties of the components (i.e., T_{c_i}, P_{c_i}, v_{c_i} are the critical temperature, pressure, and volume of component i, respectively). The constants Ω_{a_i} and Ω_{b_i} are dimensionless constants equal to 0.4278 and 0.0867, respectively, if the first and second isothermal derivatives of pressure with respect to volume are set equal to zero at the critical point. For pure substances, these constants can be evaluated by fitting the Redlich–Kwong equation to the volumetric data of saturated vapor over a temperature range that starts from the thermal boiling point to the critical point.[10] The ij subscripts refer to parameters that are characteristic of i-j interactions. Thus,

$$P_{c_{ij}} = z_{c_{ij}} R T_{c_{ij}} / v_{c_{ij}}$$

$$z_{c_{ij}} = 0.291 - 0.08[(\omega_i + \omega_j)/2]$$

$$T_{c_{ij}} = (T_{c_i} T_{c_j})^{1/2}(1 - k_{ij})$$

$$v_{c_{ij}} = [(v_{c_i} + v_{c_j})/2] \quad \text{for gases with} \quad (v_{c_i}/v_{c_j}) < 3 \quad \text{or liquids}$$

$$v_{c_{ij}}^{1/3} = [(v_{c_i}^{1/3} + v_{c_j}^{1/3})/2] \quad \text{for gases with} \quad (v_{c_i}/v_{c_j}) > 3$$

where the binary interaction coefficient k_{ij} is a measure of the deviation from the geometric mean for $T_{c_{ij}}$, which is independent of temperature, density, and composition, and is evaluated from experiments of binary interaction between components.[10] The factors ω_i and ω_j, which are a measure of acentricity or the noncentral nature of the intermolecular forces, are also needed to get an average acentric factor, which is in turn used to evaluate an average compressibility factor $z_{c_{ij}}$ by the Pitzer correlation for normal fluids.[11]

As for the liquid phase fugacity, it can be evaluated in two different ways, depending whether the component acts as a solvent (e.g., the fuel species) or as a solute (e.g., dissolved gas). For components that act as solvents, the fugacity of species i is given in terms of the mole fraction of i, X_{is}, and the standard state pure fugacity of the same component f_i°, which is the fugacity of the pure component at the system temperature and a reference pressure P°, which is usually taken to be atmospheric pressure. A nonideality quantity that is called the

activity coefficient of species i in the mixture, and denoted by γ_i°, is also used here. The closer the activity coefficients get to 1, the more ideal the liquid. The activity coefficients are discussed in detail in Ref. 10. The liquid-phase fugacity is given by

$$f_i^l = \gamma_i^\circ X_{is} f_i^\circ \exp\left(\int_{P_0}^{P} \frac{v_i^l}{RT}\,dP\right) \tag{2}$$

The exponential term on the right-hand side of Eq. (2) is called the Poynting correction factor that corrects the fugacity in very high-pressure systems.

In the liquid phase, the Jin and Borman[9] model predicts the transient behavior of the droplet by solving the heat and mass diffusion equations numerically rather than using a lumped parameter solution, which gives unsatisfactory results because of the presence of significant heat and species gradients inside the droplet. The model accounts for the phenomenon of internal circulation of the liquid within the droplet, which has been modeled by Sirignano[12] previously. To account for this phenomena, it is assumed that the circulation in the droplet follows a Hill's vortex.[13,14]

Models using the Hill's vortex solve a two-dimensional heat transfer flow problem, rather than the one-dimensional spherically symmetric one, and that requires a substantial computational effort, making it unfeasible to extend this model to practical spray computations.[15] The other approach of adjusting the transport parameters is much more feasible for spray computations, since the diffusion problem remains one dimensional by using the idea of an effective diffusivity. Internal mixing enhances the processes of heat and mass transfer inside the droplet, and the model artificially increases the heat and mass diffusivity, depending on mixing parameters. The diffusivity is increased by C[9]

$$C = 2.685 + \frac{3.02514 \times 10^{-3}}{1.9868 \times 10^{-3} + (D_{12}t/r^2)}$$

$$\text{for} \quad 4 \times 10^{-3} \le \frac{D_{12}t}{r^2} \le 1$$

$$C = 2.685 \quad \text{for} \quad \frac{D_{12}t}{r^2} \ge 1$$

where t is the instantaneous drop lifetime, and D_{12} is the binary liquid diffusivity.

Spray Model

Solving the dynamics of the fuel spray and its interaction with the gas is essential for diesel engine modeling. To describe the atomization process, the wave breakup model of Reitz[16] was adopted. This model was found to give better agreement with droplet breakup experimental results than the Taylor analogy breakup (TAB) model of KIVA-II by Liu et al.[17] Details of the TAB spray model and its application can be found in Ref. 18.

Drop parcels are injected with characteristic size equal to the nozzle exit diameter. The subsequent breakup of the parcels containing parent drops of radius a is computed by assuming that the breakup process produces children drops with $r = B_0\Lambda$, and the breakup time is $t = 3.726B_1a/\Lambda\Omega$, where Λ and Ω are obtained from a jet stability analysis. The recommended value for constant B_0 is 0.61 for diesel sprays.[16] B_1 has been found to be related to the initial disturbance level in the liquid breakup process.[19] It can be different from one injector to another. Since in the present study there is significant spray impingement on the piston surface, the drops may rebound from the walls in a highly perturbed state. To account for this phenomenon, the values for the breakup time constant are $B_1 = 60$ initially, and then $B_1 = 1.73$ after a drop parcel hits the wall. The wall impingement model considers both droplet rebound and drops that slide along the wall surface, depending on the Weber number of the colliding drop.[2]

Further modifications to the spray breakup model were made by considering the effects of the distortion of a drop on the drop's drag coefficient.[17] The drag coefficient of a distorted drop is higher than that of a spherical drop. To account for this effect, the distortion of the drops was calculated by solving the spring–mass analogy equation of the TAB model

$$\ddot{y} = \frac{2}{3}\frac{\rho_g U^2}{\rho_L r^2} - \frac{8\sigma}{\rho_L r^3}\,y - \frac{5\mu_L}{\rho_L r^2}\,\dot{y}$$

for each drop for y, where $y = 2x/r$, and x is the displacement of the pole of the drop from its equilibrium position,[18] U is the relative velocity between the drop and the gas, and ρ is the fluid density. The distortion parameter lies between the limits of a sphere ($y = 0$) and a disk ($y = 1$), with $C_D = 1.52$. A simple expression for the drag coefficient that accounts for the effect of drop distortions was used with $C_D = C_{D,\text{sphere}}(1 + 2.632y)$.[6,17]

Ignition Modeling

The low-temperature chemistry of hydrocarbon fuels controls the ignition delay in diesel combustion. In this study, the Shell model was used for ignition kinetics modeling. The model uses a reduced kinetic mechanism that contains five generic species and eight generic reactions to simulate the autoignition phenomena of hydrocarbon fuels.[20–22] The reactions and species involved in the Shell model are linked by the following simplified reaction mechanism:

$$RH + O_2 \rightarrow 2R^*K_q \tag{3a}$$

$$R^* \rightarrow R^* + P + \text{heat}\ K_p \tag{3b}$$

$$R^* \rightarrow R^* + Bf_1K_p \tag{3c}$$

$$R^* \rightarrow R^* + Qf_4K_p \tag{3d}$$

$$R^* + Q \rightarrow R^* + Bf_2K_p \tag{3e}$$

$$B \rightarrow 2R^*K_b \tag{3f}$$

$$R^* \rightarrow \text{termination}\ f_3K_p \tag{3g}$$

$$2R^* \rightarrow \text{termination}\ K_t \tag{3h}$$

where RH is the total concentration of hydrocarbon fuel (i.e., the sum of the two fuel species), R^* is the radical formed from the fuel, B is the branching agent, Q is a labile intermediate species, and P is oxidized products, consisting of CO, CO_2, and H_2O in specified proportions. The expressions for K_q, K_p, K_b, K_t, f_1, f_2, f_3, and f_4, etc., are those given by Halstead et al.[20]

Of the eight reactions just shown, reaction (3d), the transformation of Q into B, controls the ignition delay.[21] The present study considers bicomponent fuels. Accordingly, the ignition characteristics of the fuel are assumed to be given by the local cetane number (CN) (which is found from a mass-weighted linear interpolation for the two fuel species), at each point in the combustion chamber. The higher the CN, the more readily the fuel ignites, and vice versa. The local composition of the fuel determines the CN, which is used to determine the ignition rate. The activation energy of reaction (3d), E_{f4}, was modified as $E_{f4}^* = E_{f4}65/(\text{CN} + 25)$, following a correlation suggested by Heywood[23] for the effect of fuel cetane number on ignition delays in diesel engines.

Combustion

In diesel engines, a significant portion of combustion is thought to be mixing-controlled. Hence, interactions between turbulence and chemical reactions have to be considered. A laminar-and-turbulent characteristic-time combustion model

was used for the present study. The local time rate of change of the partial density of species m, resulting from the conversion from one chemical species to another, is given by

$$\frac{dY_m}{dt} = -\frac{Y_m - Y_m^*}{\tau_c} \quad (4)$$

where Y_m is the mass fraction of species m, Y_m^* is the local and instantaneous thermodynamic equilibrium value of the mass fraction, and τ_c is the characteristic time for the achievement of equilibrium. To predict thermodynamic equilibrium temperatures accurately, it is sufficient to consider seven species: fuel, O_2, N_2, CO_2, CO, H_2, and H_2O, and to assume that τ_c is the same for all seven. As was previously assumed for the ignition model, the two fuel species are combined into an effective fuel for the purposes of the combustion model.

Following the suggestion of Kong and Reitz,[21] the ignition model was used whenever and wherever the temperature was lower than 1000 K, to simulate the ignition chemistry and to locate the ignition cells. At temperatures higher than 1000 K, the autoignition reactions become very fast and, hence, the combustion model of Eq. (4) was activated for describing high-temperature conversion from fuel to products.

The time τ_c is the sum of a laminar and turbulent time scale, $\tau_c = \tau_l + f\tau_t$. The laminar time scale τ_l is derived from an Arrhenius-type reaction rate,[24] $\tau_l = A^{-1}[\text{fuel}]^{0.75}[O_2]^{-1.5} \exp(E/RT)$ with the pre-exponential constant $A = 7.68 \times 10^8$ and the activation energy $E = 77.3$ kJ/mol. The turbulent time scale τ_t is proportional to the eddy turnover time $\tau_t = C_2 k/\varepsilon$, where $C_2 = 0.1$ (Refs. 7 and 25), and k and ε are calculated from the modified renormalization group (RNG) k-ε turbulence model.[22] The delay coefficient, which is given by $f = (1 - e^{-r})/0.632$, simulates the increasing influence of turbulence on combustion after ignition has occurred, and r is the ratio of the mass of products to that of total reactive species. The parameter r indicates the completeness of combustion in a specific region. Its value varies from 0 (no combustion yet) to 1 (complete consumption of fuel and oxygen). This approach is conceptually consistent with the mixing combustion model of Magnussen and Hjertager.[26]

Results

Warm Engine Computations

Experimental results from a single-cylinder version of the Caterpillar 3406 heavy-duty diesel engine were used in this study for validation of the model calculations for a warm engine operating condition case. The engine has been well characterized in previous experimental and computational studies, including emissions measurements,[27,28] in-cylinder gas temperature,[29] gas velocity measurements,[30] and realistic intake flow computations.[31] Details of the engine specifications are given in Table 1.

The computations considered a single injection with an injection pressure of 90 MPa, with a start of injection timing of −11-deg CA ATDC (crank angle degrees after top dead center). The nozzle tip had six holes with hole diameters of 0.259 mm and an included angle between fuel sprays of 125 deg. This configuration results in significant spray impingement on the piston. The injection profile featured fast opening and closing rates (~2 crank angle degrees for opening and closing[32]), and the experimental injected mass flow rates were used to compute the injection velocities for the computations. The experimental injection profile was used for both normal and cold-starting conditions. The experimental pressure data were analyzed by a heat-release analysis.[33]

Table 1 Caterpillar engine specifications and standard warm operating conditions

Bore, 137.19 mm
Stroke, 165.1 mm
Connecting rod length, 261.62 mm
Displacement, 2.44 L
Compression ratio, 15.0
Piston crown, Mexican hat
Engine speed, 1600 rpm
Intake pressure, 184 kPa
Intake temperature, 310 K
Fuel injected, 0.1622 g/cycle
Intake valve close timing, 147-deg BTDC[a]
Swirl ratio (nominal), 1.0

[a]Before top dead center.

The computational mesh used represents one-sixth of the combustion chamber in the engine (i.e., one spray in a 60-deg sector) for computational efficiency (see Fig. 1). Thus, the computational domain had periodic boundary conditions. There were 20 cells in the radial direction, 30 cells in the azimuthal direction, and 18 cells in the axial direction with 5 cells in the squish region at top dead center. Previous results indicate that the computations are most sensitive to the grid resolution in the azimuthal direction, and the present resolution was found to give adequately grid-independent results.[22,34] Typical computer times were about 2–3 Cray Y-MP hours for each run.

The fuel used in the experiment was Amoco Premier no. 2, which was modeled using a cetane/isocetane blend. The blend cetane number was determined by the percentage of isocetane in the fuel injected. It is important to note that the cetane numbers used in the ignition model are the local values of cetane numbers within the engine, since the two components vaporize at different rates because of their volatility differentials. A fuel with a cetane number of 40 is considered to be the reference fuel that is representative of the diesel fuel.

Figure 2 shows the computed cylinder pressure together with the experimental pressure trace. The CN = 40 case agrees well with the experiment, with ignition taking place at −3-deg CA. Other computations were made to assess the effect of cetane number on the results. The CN = 45 case is very similar to the CN = 40 case, but ignition takes place slightly earlier

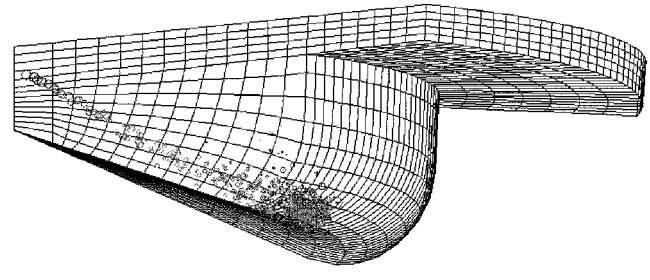

Fig. 1 Perspective view of computational grid and fuel droplet distribution at TDC.

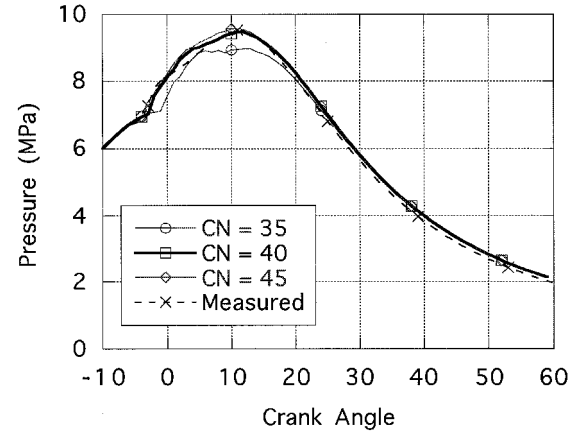

Fig. 2 Engine cylinder pressure for CN = 35, 40, and 45, with experimental data for CN = 40.

Table 2 Engine cases and ignition results with CA when gas first reaches the indicated temperatures

Case	T_{air}, K	Injection, deg	Residual	CA T = 1000 K	CA T = 1500 K	CA T = 2000 K
1	273	10.75	0% 1F	10.02	10.08	15.50
2	273	10.75	10% 1F	5.75	6.64	>6.64
3	273	21.50	10% 1F	14.05	17.46	>17.46
4	273	10.75	5% 1F	6.85	7.23	8.23
5	254	10.75	10% 1F	9.02	10.86	13.09
6	254	10.75	10% 2F	−1.36	0.70	2.02

at −4-deg CA. With a CN = 35 fuel, the ignition occurred at −0.5-deg CA and a lower peak pressure was predicted. The trend of increased ignition delay as the cetane number is decreased from 45 to 35 is consistent with the expected fuel result.[23]

Cold-Starting Conditions

The present computer model has been applied to the same engine described previously, but under cold-starting conditions.[35] The cases considered in the study are listed in Table 2. The results of these cases show that the details of the vapor fuel distribution in the engine have a significant impact on engine cold-starting.

The cases in Table 2 incorporate two main differences in the operating conditions (other than the ambient temperature, which is also assumed as the initial temperature in the engine). The first difference is that the engine speed is significantly lower than at the warm engine conditions and the cranking engine speed is variable. Experimental measurements during cold-starting show reductions in the engine speed during the compression stroke as the piston approaches top dead center (TDC).[36] For the present computations, the engine speed was assumed to follow a sine wave profile with rpm = 100 − 50 sin(CA + 90).

The other difference is that the intake pressure is atmospheric pressure rather than turbocharged. The rest of the parameters that were changed are listed in Table 2. The cases listed include two intake air temperatures, 273 K (cases 1–4) and 254 K (cases 5–9). Lower intake air temperature cases (241 K) were investigated and ignition did not occur because of the long ignition delay.[4]

It has been shown that advancing injection timing helps ignition under cold-starting conditions, since the fuel droplets do not atomize as they would under warm conditions, and thus vaporization is constrained by diffusion.[4] The start of injection was maintained at −11-deg CA ATDC (the standard start of injection), but the duration of injection was halved to 10.75 deg, except for case 3 where the standard duration of injection was used. This has the effect of increasing droplet atomization by increasing the velocity of the injected droplets.

Engine experiments show that the engine under cold-starting conditions may skip several cycles between firings with a defined frequency.[37] This can be explained by the accumulation of residual fuel inside the cylinder from nonfiring cycles until the amount of fuel reaches a certain level, and this helps to fire the engine. Based on this observation, a homogeneously distributed fuel vapor residual was introduced at intake valve closure to help start ignition. As shown in Table 2, there are cases with no residual, and cases where the intake included 10 and 5% of the total injected fuel amount as a vapor fuel residual. Among these cases the composition of the residual was changed from 100% isocetane (the cases denoted by 1F) to 40% isocetane/60% cetane (the cases denoted by 2F). This was important in the study to assess the effects of fuel composition on ignition.

The computed cylinder pressure results of these cases are displayed in Figs. 3 and 4. Although ignition started in case 1, combustion did not develop significantly, as seen in Fig. 3. The effect of the 10% residual fuel is evident in cases 2 and

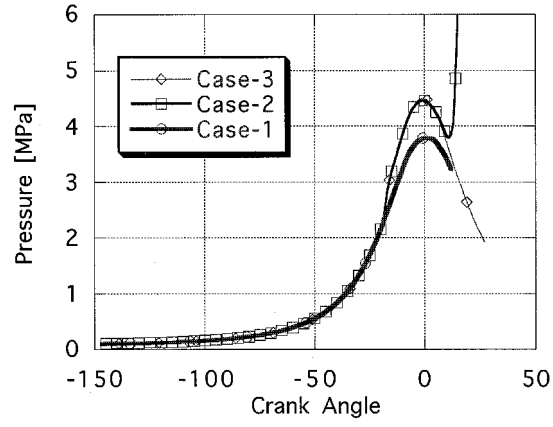

Fig. 3 Engine cylinder pressure for cases 1–3 (see Table 2).

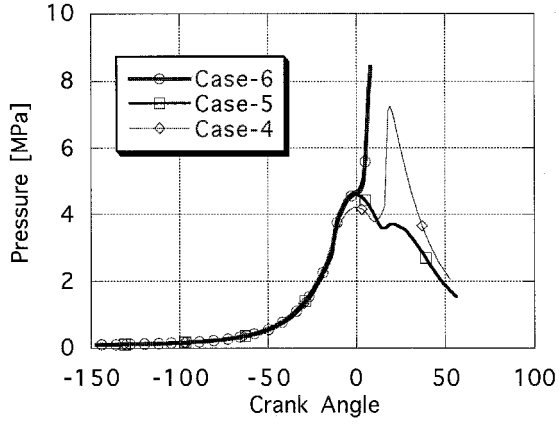

Fig. 4 Engine cylinder pressure for cases 4–6 (see Table 2).

3, as the top dead center pressure is higher in these two cases because of the initial heat release from the residual fuel. In either case, ignition did not happen while the spray was being injected, since the temperature resulting from the oxidation of the residual fuel was below 1000 K, the switchover temperature from the ignition low-temperature kinetics model to the combustion model. Thus, the residual fuel did not directly alter the combustion in the engine, but it helped accelerate ignition, as is evident in case 2. The results are also summarized in the last three columns of Table 2, which gives the crank angles where temperatures of 1000, 1500, and 2000 K are first reached somewhere in the cylinder.

The effect of increasing the duration of injection was significant, as seen in the case 3 results in Table 2, as well as in Fig. 3. With the longer injection duration (i.e., lower injection velocities), ignition occurred 10 deg later and combustion did not develop compared to case 2. This is explained by the poorer atomization that resulted from the lower injection velocities. The lower velocities and the larger droplets both reduce the amount of vaporized fuel.

Reducing the amount of residual fuel to 5% of the total injected fuel amount resulted in partial combustion in case 4,

Table 3 Engine cases and ignition results for split and continuous injections with crank angles when gas first reaches the indicated temperatures

Case	Start of injection, deg	Duration of injection, deg	CA T = 1000 K	CA T = 1500 K	CA T = 2000 K
Standard	−8.5	21.5	——	——	——
Early	−25	21.5	6.69	10.69	15.53
Split (25–75)	−25/−2	7/15	3.65	4.5	5.82

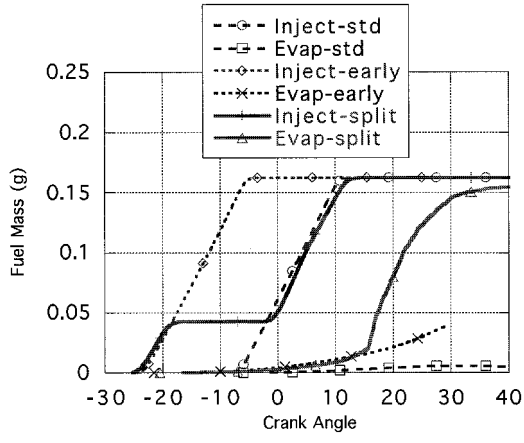

Fig. 5 History of injected and vaporized fuel for standard, split, and early injection cases.

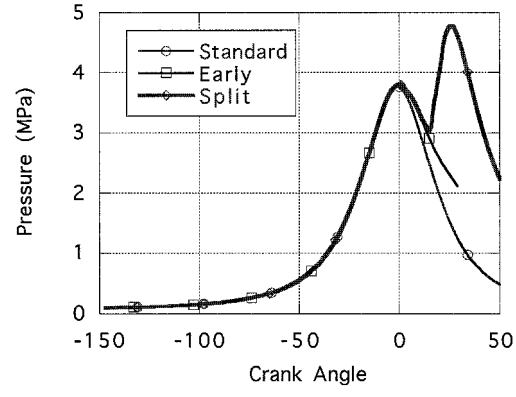

Fig. 6 Engine cylinder pressure for standard, split, and early injection cases.

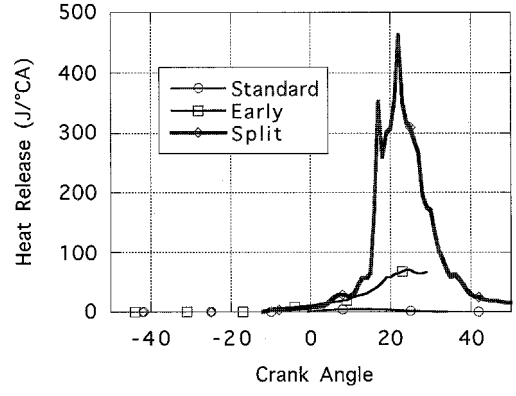

Fig. 7 Heat release rate for standard, split, and early injection cases.

as shown in Fig. 4. Although the onset of ignition was not changed appreciably by using a 5% residual instead of 10% (cases 4 and 2, respectively), the speed and progress of the combustion was significantly reduced in case 4 when compared to that of case 2. This demonstrates the importance and impact of a small percentage of the fuel charge that is carried over from one cycle to the following cycle during cold-starting. This also motivates the idea of exploring split injections, which is presented in the next section.

The ambient temperature also has a significant impact on engine performance. When the ambient air intake temperature was reduced from 273 to 254 K in cases 2 and 5, respectively, ignition was delayed and there was very little combustion, even with the presence of 10% residual fuel as seen in case 5. However, when the composition of the residual fuel was changed to include more cetane, which has a higher cetane number, and therefore, a higher tendency to ignite, ignition occurred just before top dead center and combustion started to develop at a rapid pace, as seen in case 6 in Fig. 4. This change in engine performance also demonstrates the impact of fuel composition on ignition and combustion in the engine.

Effect of Split Injections on Cold-Starting

Based on the earlier finding of the importance of residual fuel on engine performance, it was conjectured that split injections could be an effective approach to improve engine startability. In this case, a pilot injection is injected into the engine early in the compression stroke. By doing so, the fuel that is introduced to the engine in the pilot injection has sufficient time to vaporize, since the vaporization of the fuel is relatively slow under cold-starting conditions, compared to the standard engine operating conditions. Also, small amounts of fuel injected would not result in extensive cooling of the combustion chamber gas caused by vaporization, which may further slow down the ignition chemistry.

Three cases were investigated with an ambient air and initial engine temperature of 273 K, as summarized in Table 3. First, is a standard case where the start and duration of injection were −8.5- and 21.5-deg CA, respectively. The second case involved a 25% pilot injection starting at −25-deg CA, and the start of the main injection (the remaining 75% of the fuel) matches that of the standard case. The third case had one injection starting at −25-deg CA. The history of the injected and evaporated fuel is shown in Fig. 5. As can be seen, split and early injection cases had much higher vaporization rates than the standard case.

Figures 6 and 7 show the pressure and heat release, respectively, for the three different injection cases. With the standard injection, the engine misfires, and the pressure drops rapidly after TDC, as shown in Fig. 6. On the other hand, in the split and early injection cases, the pressure is higher, indicating the start of combustion and significant heat release. In particular, the pressure rise in the split injection case shows very strong combustion, indicating good startability. The heat release history shown in Fig. 7 shows the difference between the early and split injection cases, with the heat release proceeding at a much faster rate in the split injection case. This is because of the earlier ignition that started at 3.6-deg ATDC with split injection, compared to the early injection case where ignition only started at 6.7-deg ATDC, as seen in Table 3. Therefore, by adjusting the timing and amount of the pilot injection, the ignition timing can be adjusted to optimize startability.

Figures 8 and 9 show in-cylinder details for the early and split injection cases following ignition. In the case of early injection, the fuel droplets accumulate near the head and the squish region, since the droplets slide along the piston bowl

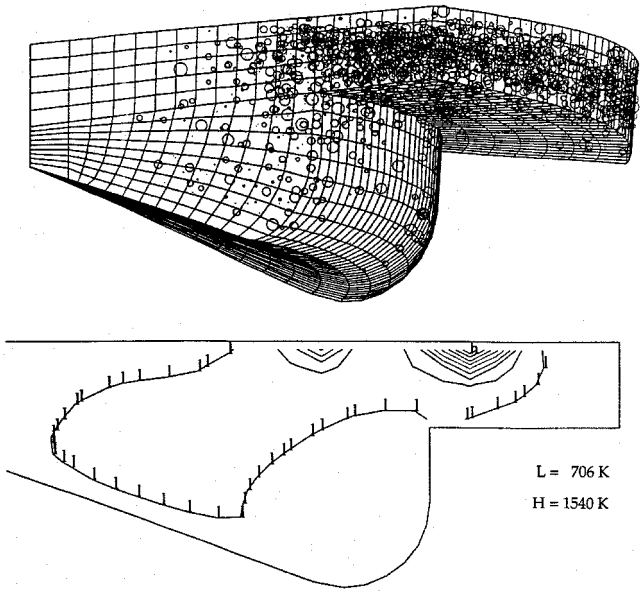

Fig. 8 Droplet distribution (at 18-deg ATDC) and temperature contours near ignition for early continuous injection case (Table 3).

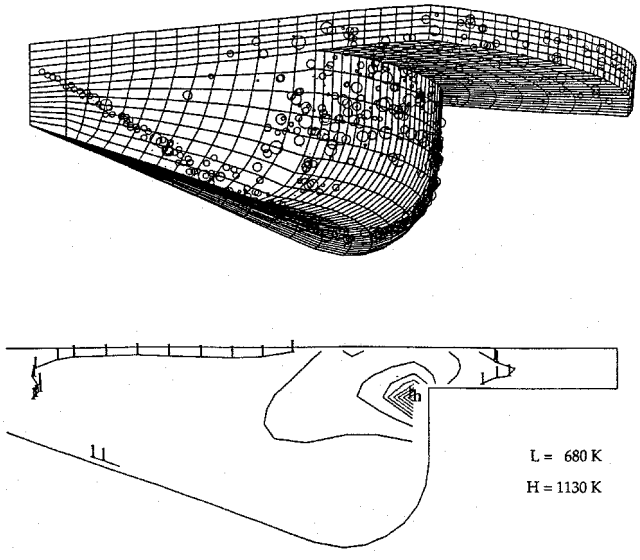

Fig. 9 Droplet distribution (at 4-deg ATDC) and temperature contours near ignition for split injection case (Table 3).

surface, as seen in Fig. 8. The temperature contours for the same case show ignition taking place just below the head in the squish region after the injection is already completed. On the other hand, ignition occurs much earlier in the split injection case, as seen in Fig. 9. Also, it takes place close to the edge of the piston bowl, while the main injection is still continuing. This results in better vaporization rates for the injected fuel droplets since the droplet vaporization will not be localized, as seen in Fig. 8.

The reason for the improved performance with split injection is also related to the fact that the spray droplets from the first injection decelerate between the two injections, creating a relatively stagnant flow in the spray region.[38] The absence of a high convective flow in the spray region promotes the development of locally high fuel vapor concentrations, which have sufficient time for the acceleration of the ignition process. In conclusion, the present results indicate that split injections can significantly improve cold-starting in diesel engines.

Conclusions

An improved version of the multidimensional computer code, KIVA-II, has been used to study the effects of multicomponent fuel vaporization on diesel engine ignition under cold-starting conditions. Improvements to the code include the implementation of a high-pressure multicomponent fuel spray vaporization model that is necessary to model real fuels in a more representative way. The model has been applied to sprays, together with improved atomization and drop breakup models, a drop drag model that accounts for drop distortions, and a spray/wall impingement model with enhanced breakup of impinging drops. For diesel engine computations, ignition was computed with a multistep kinetics ignition model that included fuel (cetane number) effects and a laminar-and-turbulent characteristic-time combustion model. The engine calculations also included a wall heat transfer model that accounts for compressibility, unsteadiness, and a piston–ring–pack crevice flow model.

The warm engine results show good agreement between measured and predicted cylinder gas pressures for standard conditions. The model was then used to study the effects of injection timing, intake air temperature, and fuel residual under cold-starting conditions. The predicted cold-starting trends are reasonable and include cases with fully developed combustion and other cases with borderline ignition. A small amount of vapor fuel residual existing in the combustion chamber was shown to enhance ignition and combustion. In addition, the composition of the residual fuel vapor was found to influence ignition. Good atomization of the spray was also shown to shorten the ignition delay. The present study shows that split injections can significantly improve cold-starting in diesel engines. In this case, a small fraction of the fuel is injected early in the compression stroke to help ignition in the same way fuel residual enhances the ignition process.

Acknowledgments

This work was supported under the Department of Energy/NASA Lewis Research Center Grant NAG 3-1087, and by the U.S. Army Research Office Grant DAA404-94-G-0328. Support for the computations was provided by Cray Research, Inc.

References

[1]Henein, N. A., and Lee, C. S., "Autoignition and Combustion of Fuels in Diesel Engines Under Low Ambient Temperatures," Society of Automotive Engineers, Paper 861230, 1986.

[2]Gonzalez, M. A., Borman, G. L., and Reitz, R. D., "A Study of Diesel Cold Starting Using Both Cycle Analysis and Multidimensional Computations," Society of Automotive Engineers, Paper 910180, 1991.

[3]Lefebvre, A. H., *Atomization and Sprays*, Hemisphere, New York, 1989.

[4]Ayoub, N. S., and Reitz, R. D., "Multidimensional Computation of Multicomponent Spray Vaporization and Combustion," Society of Automotive Engineers, Paper 950285, 1995.

[5]Amsden, A. A., O'Rourke, P. J., and Butler, T. D., "KIVA-II—A Computer Program for Chemically Reactive Flows with Sprays," Los Alamos National Labs., LA-11560-MS, Los Alamos, NM, 1989.

[6]Kong, S. C., and Reitz, R. D., "Spray Combustion Processes in Internal Combustion Engines," *Recent Advances in Spray Combustion*, edited by K. K. Kuo, AIAA Education Series, AIAA, Reston, VA, 1996.

[7]Reitz, R. D., "Assessment of Wall Heat Transfer Models for Premixed-Charge Engine Combustion Computations," Society of Automotive Engineers, Paper 910267, 1991.

[8]Reitz, R. D., and Kuo, T. W., "Modeling of HC Emissions Due to Crevice Flows in Premixed-Charge Engines," Society of Automotive Engineers, Paper 892085, 1989.

[9]Jin, J. D., and Borman, G. L., "A Model for Multicomponent Droplet Vaporization at High Ambient Pressures," Society of Automotive Engineers, Paper 850264, 1985.

[10]Prausnitz, J. M., and Chuen, P. L., *Computer Calculations for High-Pressure Vapor-Liquid Equilibria*, Prentice–Hall, Englewood Cliffs, NJ, 1968.

[11]Prausnitz, J. M., *Molecular Thermodynamics of Fluid-Phase*

Equilibria, Prentice–Hall, Englewood Cliffs, NJ, 1969.

[12]Sirignano, W. A., "Fuel Vaporization and Spray Combustion Theory," *Progress in Energy and Combustion Science*, Vol. 9, 1983, pp. 291–322.

[13]Tong, A. Y., and Sirignano, W. A., "Multicomponent Transient Droplet Vaporization with Internal Circulation: Integral Equation Formulation and Approximate Solution," *Numerical Heat Transfer*, Vol. 10, No. 3, 1986, pp. 253–278.

[14]Renksizbulut, M., and Yuen, M. C., "Numerical Study of Droplet Evaporation in a High Temperature Stream," *Journal of Heat Transfer*, Vol. 105, No. 2, 1983, pp. 389–397.

[15]Tong, A. Y., and Sirignano, W. A., "Analytical Solution for Diffusion and Circulation in a Vaporizing Droplet," *Proceedings of the 19th Symposium (International) on Combustion*, The Combustion Inst., Pittsburgh, PA, 1982, pp. 1023–1041.

[16]Reitz, R. D., "Modeling Atomization Processes in High-Pressure Vaporizing Sprays," *Atomization and Spray Technology*, Vol. 3, No. 4, 1987, pp. 309–337.

[17]Liu, A. B., Mather D., and Reitz, R. D., "Modeling the Effects of Drop Drag and Breakup on Fuel Sprays," Society of Automotive Engineers, Paper 930072, 1993.

[18]O'Rourke, P. J., and Amsden, A. A., "The TAB Method for Numerical Calculation of Spray Droplet Breakup," Society of Automotive Engineers, Paper 872089, 1987.

[19]Liu, A. B., and Reitz, R. D., "Mechanism of Air-Assisted Liquid Atomization," *Atomization and Sprays*, Vol. 3, No. 1, 1993, pp. 55–75.

[20]Halstead, M., Kirsh, L., and Quinn, C., "The Autoignition of Hydrocarbon Fuels at High Temperatures and Pressures—Fitting of a Mathematical Model," *Combustion and Flame*, Vol. 30, 1977, pp. 45–60.

[21]Kong, S. C., and Reitz, R. D., "Multidimensional Modeling of Diesel Ignition and Combustion Using a Multistep Kinetics Model," *Journal of Engineering for Gas Turbines and Power*, Vol. 115, No. 4, 1993, pp. 781–789.

[22]Kong, S. C., Han, Z., and Reitz, R. D., "The Development and Application of a Diesel Ignition and Combustion Model for Multidimensional Engine Simulations," Society of Automotive Engineers, Paper 950278, 1995.

[23]Heywood, J. B., *Internal Combustion Engine Fundamentals*, McGraw–Hill, New York, 1988.

[24]Bergeron, C. A., and Hallett, W., "Ignition Characteristics of Liquid Hydrocarbon Fuels as Single Droplets," *Canadian Journal of Chemical Engineering*, Vol. 67, No. 1, 1989, pp. 142–149.

[25]Kong, S. C., Ayoub, N., and Reitz, R. D., "Modeling Combustion in Compression Ignition Homogeneous Charge Engines," Society of Automotive Engineers, Paper 920512, 1992.

[26]Magnussen, B. F., and Hjertager, B. H., "On Mathematical Modeling of Turbulent Combustion with Special Emphasis on Soot Formation and Combustion," *16th Symposium (International) on Combustion*, The Combustion Inst., Pittsburgh, PA, 1976, pp. 719–729.

[27]Nehmer, D. A., "Measurement of the Effect of Injection Rate and Split Injections on Diesel Engine Soot and NOx Emissions," M.S. Thesis, Univ. of Wisconsin, Madison, WI, 1993.

[28]Tow, T., Pierpont, A., and Reitz, R. D., "Reducing Particulates and NO_x Emissions by Using Multiple Injections in a Heavy Duty D.I. Diesel Engine," Society of Automotive Engineers, Paper 940897, 1994.

[29]Giangregorio, R. P., Zhu, Y., and Reitz, R. D., "Application of Schlieren Optical Techniques for the Measurement of Gas Temperature and Turbulent Diffusivity in a Diesel Engine," Society of Automotive Engineers, Paper 930869, 1993.

[30]Sweetland, P., and Reitz, R. D., "Particle Image Velocimetry Measurements in the Piston Bowl of a DI Diesel Engine," Society of Automotive Engineers, Paper 940283, 1994.

[31]Rutland, C. J., Pieper, C., and Hessel, R., "Intake and Cylinder Flow Modeling with a Dual-Valve Port," Society of Automotive Engineers, Paper 930069, 1993.

[32]Nehmer, D. A., and Reitz, R. D., "Measurement of the Effect of Injection Rate and Split Injections on Diesel Engine Soot and NO_x Emissions," Society of Automotive Engineers, Paper 940668, 1994.

[33]Tree, D., "Soot Particle Size and Number Density Measurements in a Direct Injection Diesel Engine Using Light Scattering, Radiation, and Extinction," Ph.D. Dissertation, Univ. of Wisconsin, Madison, WI, 1992.

[34]Patterson, M. A., Kong, S. C., Hampson, G. J., and Reitz, R. D., "Modeling the Effects of Fuel Injection Characteristics on Diesel Engine Soot and NO_x Emissions," Society of Automotive Engineers, Paper 940523, 1994.

[35]Ayoub, N. S., "Modeling Multicomponent Fuel Sprays in Engines with Application to Diesel Cold-Starting," Ph.D. Dissertation, Univ. of Wisconsin, Madison, WI, 1995.

[36]Poublon, M., Patterson, D., and Boerma, M., "Instantaneous Crank Speed Variations as Related to Engine Starting," Society of Automotive Engineers, Paper 850482, 1985.

[37]Henein, N. A., and Zadeh, A., "Diesel Cold Starting: Actual Cycle Analysis Under Borderline Conditions," Society of Automotive Engineers, Paper 900441, 1990.

[38]Han, Z., Uludogan, A., Hampson, G., and Reitz, R. D., "Mechanisms of Soot and NO_x Emission Reduction Using Multiple Injections in a Diesel Engine," Society of Automotive Engineers, Paper 960633, 1996.